Low force electrical switching using gold sputter coated vertically aligned multi-walled carbon nanotubes surfaces.

E.M. Yunus pgesa@soton.ac.uk
J.W. McBride J.W.Mcbride@soton.ac.uk
S.M. Spearing Spearing@ soton.ac.uk

School of Engineering Sciences, University of Southampton, SO17 1BJ, UK

Summary
Gold coated vertically aligned carbon-nanotubes (Au/MWCNT) surfaces are investigated to determine the electrical contact performance under low force conditions with repeated load cycling. The multi-walled CNT's are synthesized on silicon planar and sputter coated with a gold film. These planar surfaces are mounted on the tip of a PZT actuator and mated with a coated Au hemispherical probe. The load is typical of MEMs devices, with a 4V supply, 1 and 10mA current, and applied force of 1mN. The contact resistance (R_c) is monitored with the repeated loading cycles (over 1000 and a million cycle) to determine reliability and durability testing. The surfaces are compared with a reference Au-Au contact under the same experimental conditions. This study shows the potential for the application of CNT surfaces as an interface in low force electrical contact applications.

Key words:
contact force, contact resistance, carbon nanotubes, and Au/multi walled carbon nanotubes.

1.Introduction

In this paper, a study of electrical contact between surfaces under low dynamic force conditions, typically 1mN was performed. Such conditions are relevant to a number of micro-contact applications, for example MEMS relay devices. There are a number of prospective materials commonly used for this application including gold, palladium and platinum [1] but they are relatively soft and wear easily. Low contact resistance of MEMS relays requires contact material with low resistivity, high wear resistance and high resistance to oxidation [2]. It is desired to have a contact resistance of less than 1~2Ω during hot switched cycles [1,3,4,5,6]. Other materials which are of interest on MEMS relay's micro-contact include silicon carbide and diamond films. Both have high moduli but high electrical resistivity. This makes them unsuitable for electrical contact applications. There have been attempts to lower the resistivity. When doping SiC film with NH3 the resistivity drops to 1 x 10^{-4} Ωm [7] and doping DLC with ruthenium the resistivity drops to 1 x 10^{-5} Ωm [8], however, both materials still have a high resistivity compared to gold and even gold alloys (for example Au-6.3% Pt has a resistivity of 7.17 x 10^{-8} Ωm)[1].

A carbon nanotube (CNT) coated surface has potential as a material for MEMS relay applications specifically as a contact material because of its excellent mechanical and electrical properties. The following mechanical properties have been determined; CNTs tensile strength of up to 63 GPa has been measured [9]. Experiments using an atomic force microscope were performed to measure the elastic modulus and bending strength of individual, structurally isolated, multi-wall carbon nanotubes and indicated values of 1.26 TPa and 14.2 GPa [10] respectively. Experiments were also conducted

on CNTs using nano-indentation apparatus and values were obtained for the bending modulus; 1.24 TPa, axial modulus; 1.23 TPa and wall modulus; 5.61 TPa [11]. Another report shows that CNT's have an elastic modulus greater than 1 TPa [12] compared to diamond, which has a modulus of 1.2 TPa.

In terms of its electrical properties, it is calculated [13] that a 4-10 μm long SWCNT with a diameter of 1.2nm has a resistivity of 0.88 x 10^{-8} Ωm and is thought to exhibit ballistic electrical conduction. The calculation is performed using the theory of ballistic conductors and it is assumed that the CNT is defect-free. In addition, if a CNT were to be filled with metal, to form a composite its resistivity would fall to $0.35x10^{-8}$ Ωm. The mechanical and electrical properties are therefore potentially comparable to diamond and gold respectively, however, as yet no experiments have been reported on CNT metal composites for micro-contact applications.

An experiment has been performed [14] using an inch-worm with nanometer linear resolution was used to control the movement of the upper and lower electrode coated with CNT. The contact resistance, R_c is measured between CNT coated electrodes in ambient air and in a vacuum. The author concluded that the contact resistance, R_c was found to be much lower in ambient air (~160 Ω) than in vacuum (>4kΩ). In a more recent experiment [15] using a microtribometer, which allows simultaneous force/displacement (~150 mN applied force) and R_c measurement between the upper and lower electrode coated with Au and CNT respectively. The Au probe is made in contact with the substrate coated with tangled single walled carbon nanotubes. The authors concluded that a tangled Single Walled Carbon Nanotube (SWCNT) film against an Au coated surface works better than two contacting tangled films.

In the present work a novel approach is used in which a CNT "forest" is over coated with gold, in order to provide a high conductivity surface layer with a compliant under layer. This paper presents a continuation of previous experimental work. In the previous work a modified nano-indentation apparatus [16] was used to determine the contact resistance, R_c, as a function of contact force and load cycling up to ten load cycles. In a more recent experiment [17] an apparatus has been designed, in which a PZT actuator is used to support planar coated surfaces and repeated switching actions up to 1000 load cycles were performed. Both experiments uses dry circuit condition and the results showed that the performance and contact resistance of Au-Au/MWCNT contact pairs is comparable to Au-Au contact pairs and during ten and 1000 load cycles of Au-Au/MWNT contact pair shows stable and constant contact resistance.

2. Material Preparation

In this study two contact pairs have been investigated; Au to Au and Au to Au/Multi Walled Carbon Nanotubes (MWCNTs) composite. The geometry selected is a 2mm diameter hemisphere probe contacting a flat surface. In all cases the hemisphere probe consists of a stainless steel base, sputter coated with Au, ~500 nm thick, with surface roughness R_a≈400nm. In the Au to Au case (Sample 1), the flat surface is a silicon (Si) substrate (~2mm by 7mm), sputter coated with Au ~500 nm, with a surface roughness R_a≈30nm.

For the Au to Au/MWCNT case (Sample 2), a "forest" of MWCNTs is grown on the Si wafer using thermal CVD. The catalyst used is sputter deposited Fe and the

gaseous carbon source is ethylene. The growth temperature and time is 875^{o}C and 3 minutes respectively to produce a dense forest of vertically aligned MWCNT of an average length of ~50μm as shown in Fig 1. Au is then sputtered on the upper surface of the MWCNT forest to produce Au/MWCNT composite coatings as shown in Fig 2, with surface roughness R_a≈1.5μm. It is shown in Fig 3, that the Au penetrates the MWCNT surface to a depth of 2-4 μm.

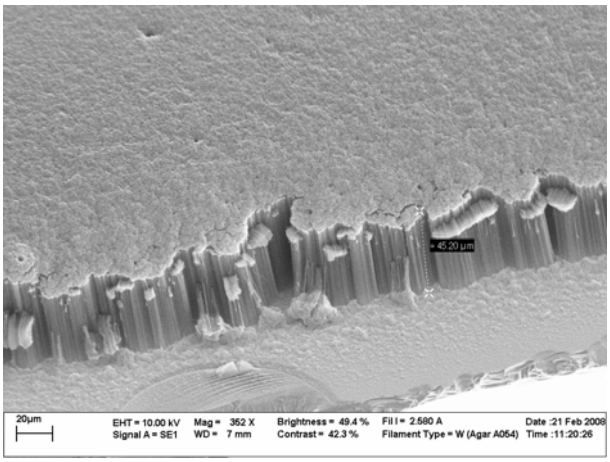

Figure 1: Dense forest of MWCNT with average length ~50μm.

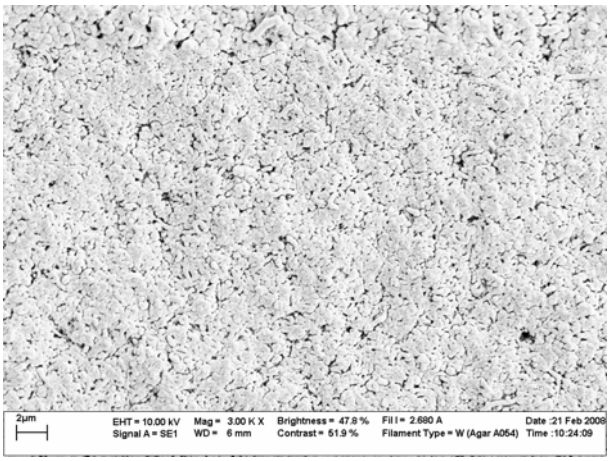

Figure 2: Sample 2, Au/MWCNT composite contact surface.

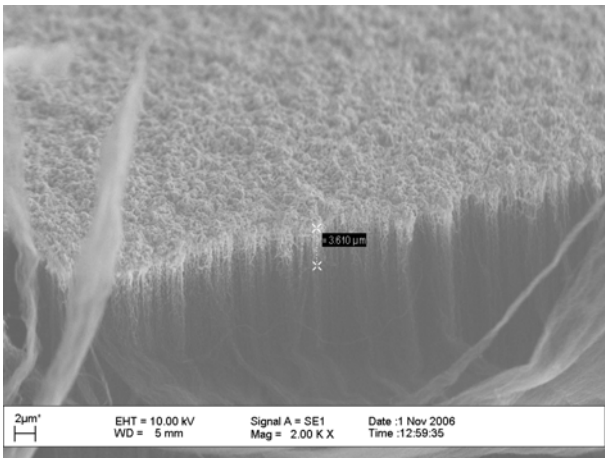

Figure 3: Au penetration on MWCNT by sputtering.

3. Experimental Method

An apparatus has been designed, in which a PZT actuator is used to support the planar coated surfaces as shown in Fig 4, to perform repeated switching actions. This surface makes electrical contact with the lower Au-coated hemispherical probe to mimic the actuation of a MEMS relay micro-contact, thus enabling the observation of the surfaces performance.

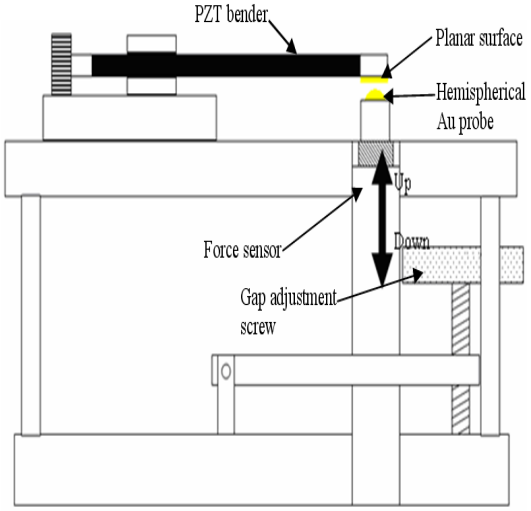

Figure 4: Schematic side view of the test rig.

A signal generator with voltage amplification is used to actuate the PZT actuator as shown in Fig 5. The PZT actuator's layers consist of Nickel (1st layer), PZT material (Lead Zirconate Titanate) (2nd layer), Nickel (3rd layer) and Kovar (Nickel-Cobalt ferrous alloy, final layer) and has a resonance frequency of ~900Hz (1st harmonic). The force sensor underneath the Au hemispherical probe is amplified using a charge amplifier and the dynamic force monitored, as shown in Fig 4 and 5.

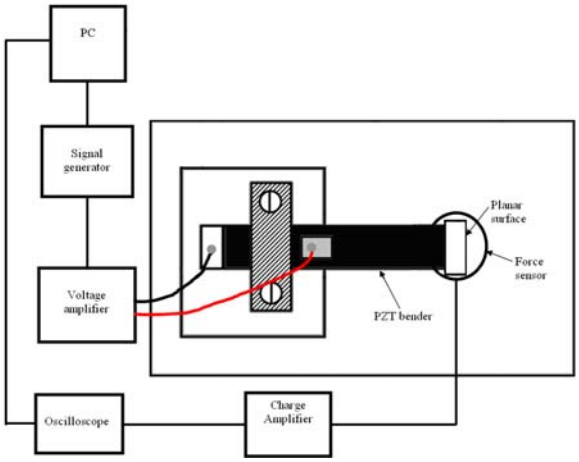

Figure 5: Schematic top view of the test system

In this experiment the PZT actuator is first actuated at low frequency (0.2Hz) to allow a quasi-static study of the contact surfaces up to 1000 cycles. The coated planar surface and Au ball are brought into contact at this frequency using an applied square wave form, and the gap between the upper and lower electrode is adjusted so that a maximum load of 1 mN is reached. In order to replicate the conditions of a MEMS relay this maximum dynamic applied force is used. Fig 6 (a) and (b) shows an example of the load history over a period of time. The current load used are 1mA and

10 mA at 4V (hot-switching). Fig 7 shows the circuit arrangement for the hot-switching experiment. After every 10th cycles the current and supply load is switched off and the contact resistance, R_c is measured using the 4 wire-measurement methods as shown in Fig 7.

The next experiment is by actuating the PZT actuator at a higher frequency (10 Hz) to study the contact surfaces over a million cycles as shown in Fig 8. Fig 8 (a) and (b) shows an example of the load history over a period of time at 10Hz. Same applied load, current and supply load is used during hot-switching. The R_c is measured at during quasi-static frequency (0.2Hz) actuation and using 4-wire measurement methods, after 3000, 6000, 9000, 10000, 300000, 865000, and over a million cycles. At 0.2Hz, for both experiment the targeted load is applied for ~3 seconds so that a representative average contact resistance value can be determined [17]. During the hot-switching current and supply load for both experiments in use is a typically used for MEMS RF switches. Thus, the high current range and supply range are represented [18,5,22,19].

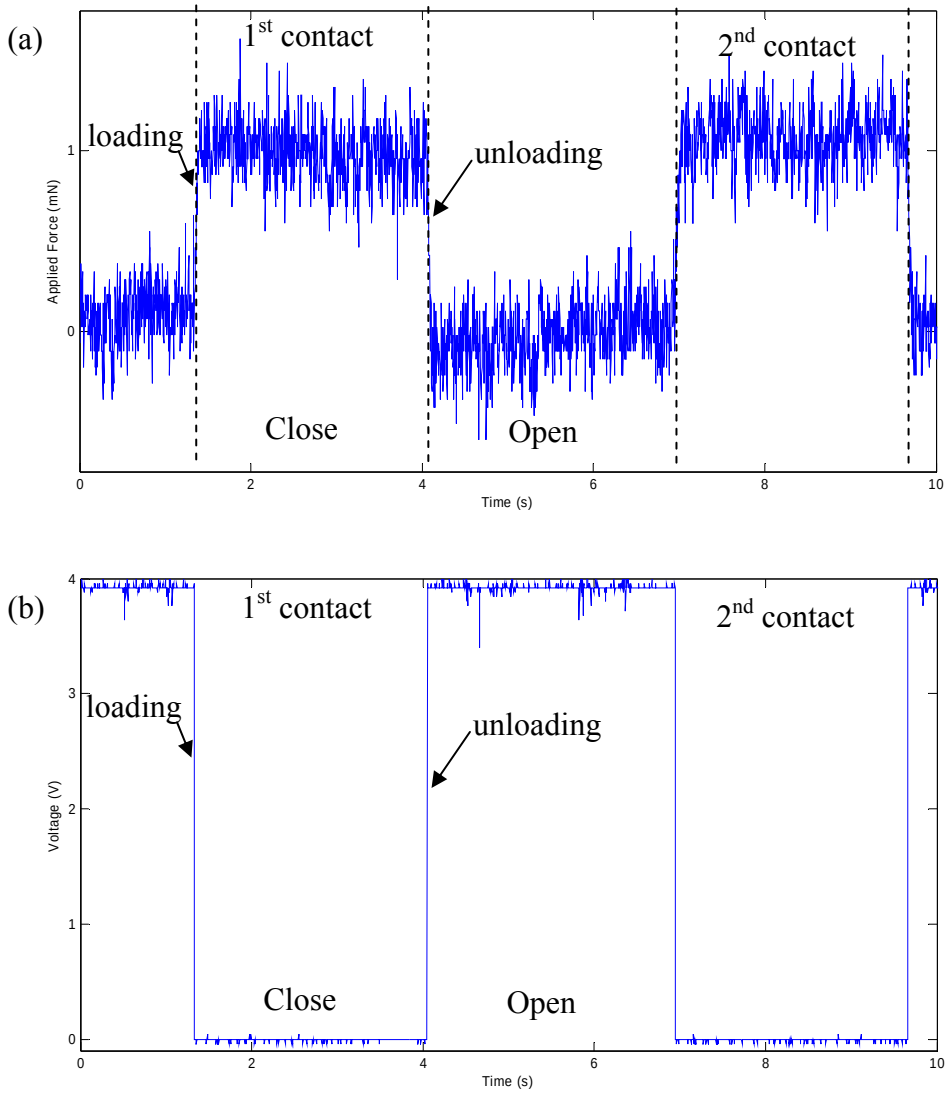

Figure 6(a) Example of applied force against time at 1mN, 0.2Hz for Au-Au contact pair (b) example of voltage against time for 1mN applied force at 1mA/4V (0.2Hz) for Au-Au contact pair.

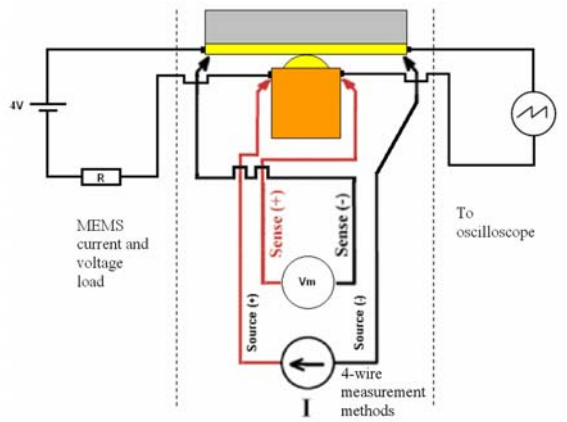

Figure 7: Schematic of contact zone with its electrode, current and supply load, 4 wire measurement and the monitoring.

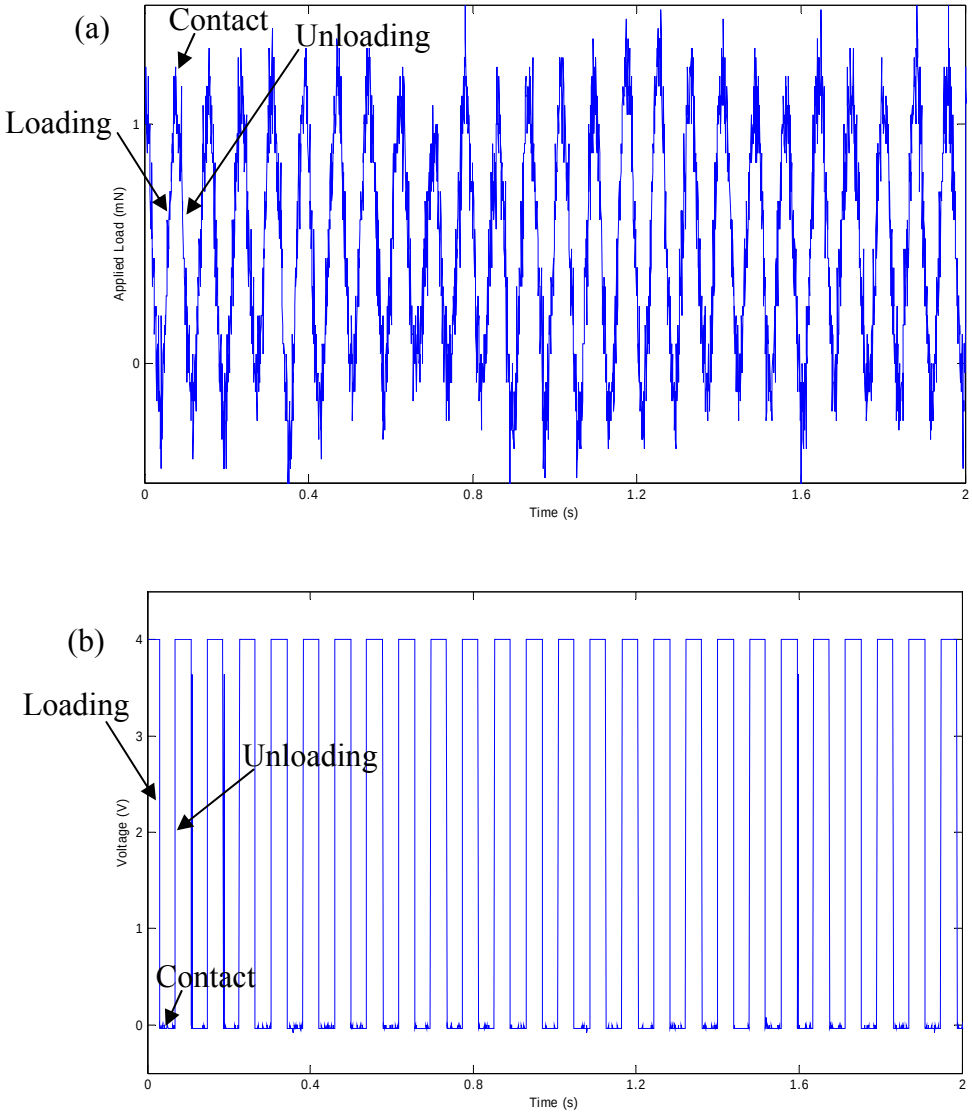

Figure 8: (a) Example of applied load against time for Au-Au contact pair at 10 Hz (b) example of voltage against time for Au-Au contact pair at 10Hz.

The apparatus is enclosed and held at ambient air and room temperature. The aim of this study is to determine the stability, reliability and durability of the contact surfaces, prior to longer duration testing under variable MEMS current load conditions. The performance of the Au-Au/MWCNT surfaces is compared to a reference Au-Au contact pair under the same experimental conditions in order to assess their mechanical and electrical stability and reliability. SEM image, TaiCaan Technologies XYRIS 4000L laser scanner and X-ray spectroscopy are used to confirm any changes on the contact surfaces samples such as degradation and wear.

4. Results and Discussion

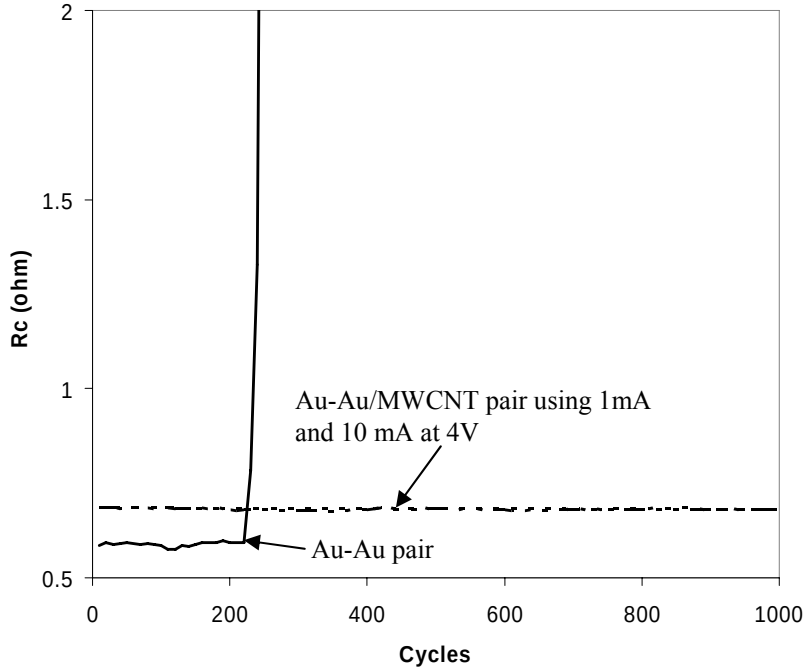

Figure 9: Cyclic contact resistance for Au-Au and Au-Au/MWCNT contact pair.

Fig 9 shows the contact resistance of Au-Au pair over 1000 cycles at a maximum (quasi static) applied load of 1mN. The contact resistance of the Au-Au pair is initially ~0.58Ω and increases rapidly to 4-10Ω at ~220 cycles. The reason for the sharp increase in R_c of Au-Au pair is due to the melting and smoothening of the Au surfaces which leads to increased adhesion [18, 20]. The melting is due the voltage load (4V) used in this experiment, where the theoretical voltage for melting Au contact material is ~0.43V [21]. The smoothing is the result of the repeated impacts and time-dependent deformation of the Au. This can be seen in Fig 10 (a) and (b) which shows the damaged Au hemispherical probe surface and adhered Au on the Au planar for the Au-Au contact pair respectively. Fig 10 (c) also shows scanned image of the damaged Au hemispherical probe using TaiCaan (Xyris 4000CL). The damage depth measured is ~500nm, thus exposing the under layer.

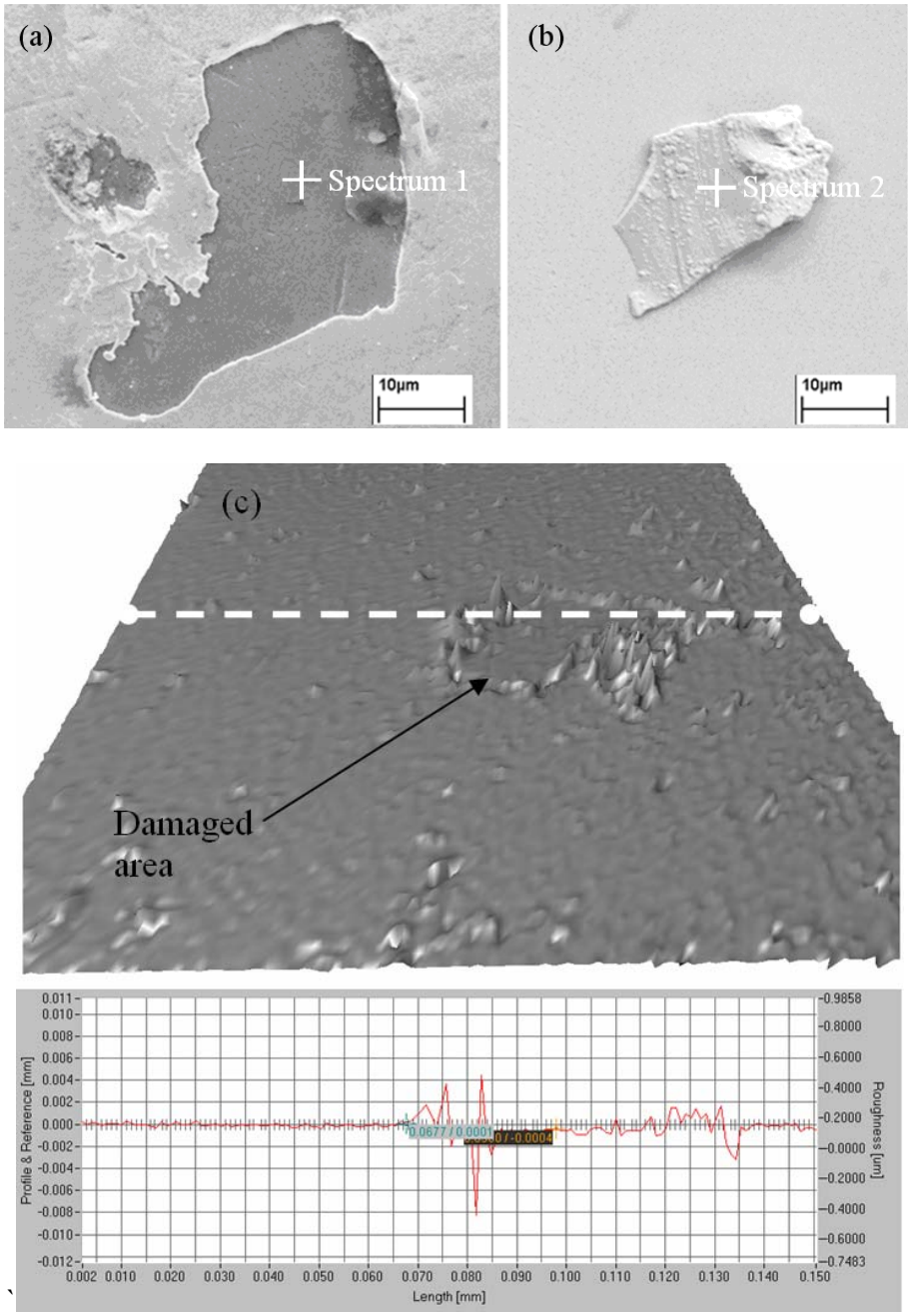

Figure 10: (a) SEM image of Au hemispherical probe degradation (b) SEM image of Au planar with Au debris (c) Scanned image of damaged Au ball for Au-Au pair (1mA/4V) with the sphere removed, contact pair 201x201 (0.2mmx0.2mm) using TaiCaan (Xyris 4000CL).

This can be confirmed using X-ray spectroscopy. Fig 10 (a) shows the point analysed by X-ray spectroscopy on the Au hemispherical probe "Spectrum 1". Fig 11 (a) shows an EDX spectrum for the surface. The 'Fe' peak was predominantly observed and Cr peak indicates both elements come from the stainless steel ball. The atomic percent shows Fe is 73.21% and Cr is 26.29% thus indicating that wear and damage has occurred on the Au hemispherical probe exposing the surface of the ball. Fig 10 (b) also shows the point analysed by X-ray spectroscopy of the adhered Au on the Au

planar “Spectrum 2”. Fig 11 (b) shows an EDX spectrum for the surface. The ‘Au’ peak was predominantly observed with Au atomic percent of 100% thus indicating that Au debris has adhered on the Au planar.

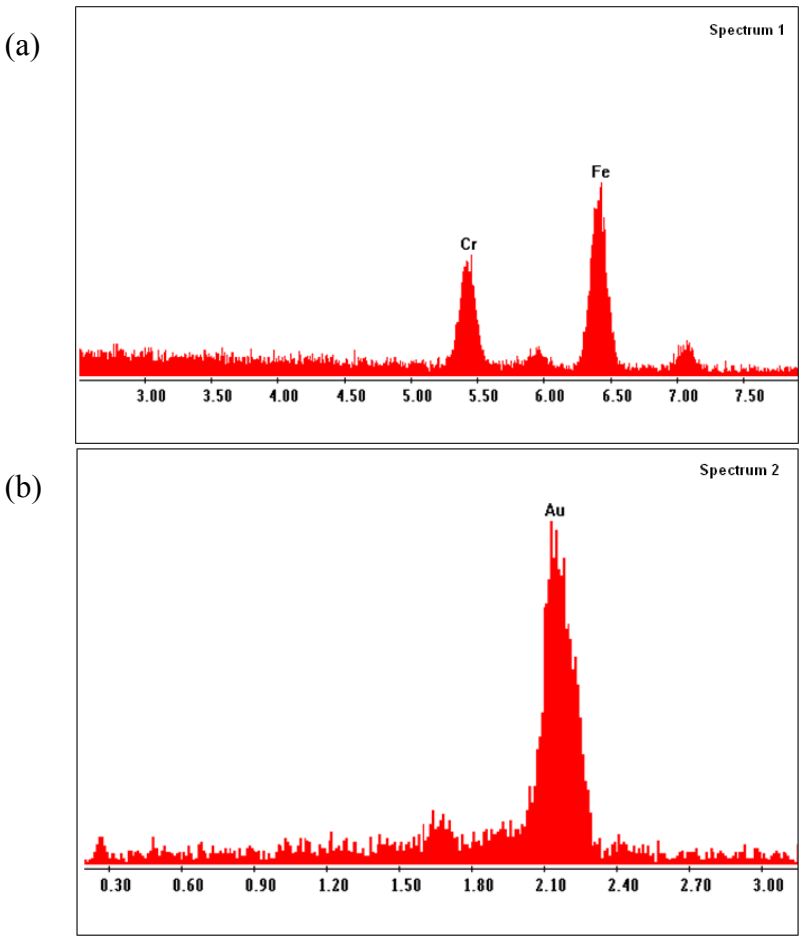

Figure 11: (a) EDX spectrum of exposed under layer of Au hemispherical probe surface (b) EDX spectrum of adhered Au on the Au planar surface.

To explain this further, a recent experiment [22] using a modified nano-indentation apparatus shows the Au-Pt contact pair degrading and the contact resistance increases after the 10th cycle. It was proposed that this is due to hot-switched contact conditions (3.3V and 3mA). In an another experiment [16] using a nanoindentation apparatus but for Au-Au contact pair using dry circuit condition shows creep occur during a single load cycle, as shown in Fig 12. In this experiment the diamond indenter is replaced with Au hemispherical probe. The adhesive force increases with the number of cycles and it is consistent with creep being one of the underlying physical mechanisms for the increase in adhesion [20].

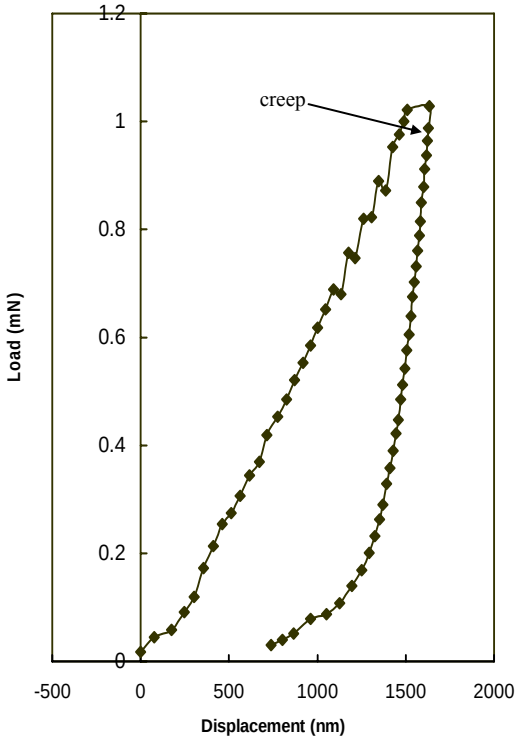

Figure 12: Graph of load against displacement for Au-Au contact pair.

Fig 9 also shows contact resistance of Au-Au/MWCNT contact pair at different current load (1mA and 10mA) at 4V. The contact resistance (~0.68Ω) for both current load conditions is slightly higher for the Au-Au/MWNT pair when compared with Au-Au pair (~0.58Ω). The likely cause is the difference of surface roughness between Au and Au/MWCNT coated planar surface. The contact resistance is much more stable than for the Au-Au pair over 1000 loading cycles. This is believed to be due to the deformation required to form the contact being provided by elastic deflection of the MWCNTs rather than plastic deformation of the Au surface. The MWCNT's provide elastic deformation is supported by the results in [11] where the use of nanoindentation apparatus with a diamond indenter performed indentation on a planar surface coated with vertically aligned CNT was investigated. It was shown that the CNTs deflected elastically as the diamond tip indented the surface layer.

A graph of load against displacement using nanoindention apparatus with Au-MWCNT pair as shown in Fig. 13 shows that MWCNTs are elastic [16]. The curve in Fig 13 shows that there is much less permanent displacement (region 1) once the indentation load is removed. This is consistent with the MWNT deforming elastically whereas the Au surface on both the hemispherical probe and planar undergoes plastic deformation (region 2) for Au-Au/MWCNT pair. In [16] also shows an SEM image of the Au hemispherical probe contact surface after the load cycles having some damage to the Au surfaces where many small impressions on the Au hemispherical probe are detected. These impressions are due to the asperities on the MWNT surfaces. Moreover when the surface roughness (R_a) is measured in this region it has changed from ~400 nm to ~1.5μm.

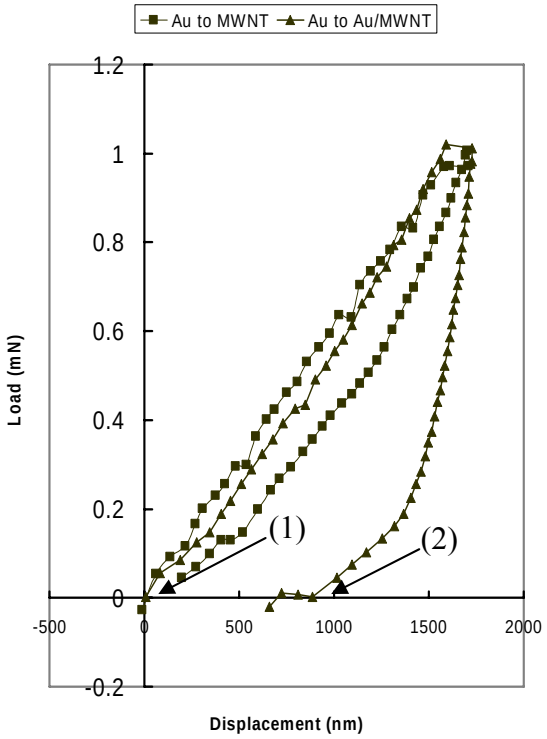

Figure 13: Graph of load against displacement for Au-MWCNT and Au-Au/MWCNT pair.

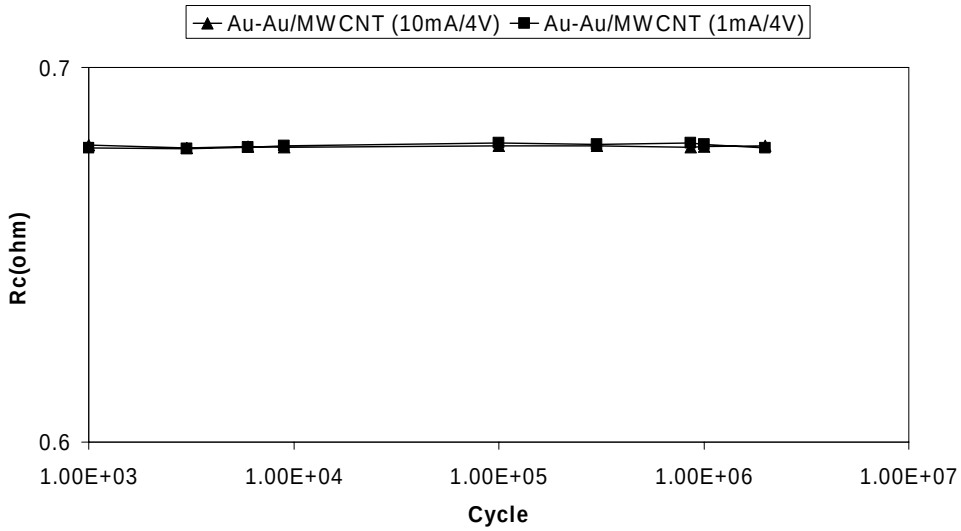

Figure 14: Contact resistance up to more than 1 million cycles for Au-Au/MWCNT contact pair.

Fig 14 shows the contact resistance over a million cycles. The contact resistance is stable for both current load (1mA and 10mA) conditions. Even though there are some Au adhesion on the Au hemispherical probe as shown in Fig 15 (a) and (b). This Au adhesion is from the coated surface of the Au/MWCNT planar surfaces, which melted and adhered onto the Au hemispherical probe.

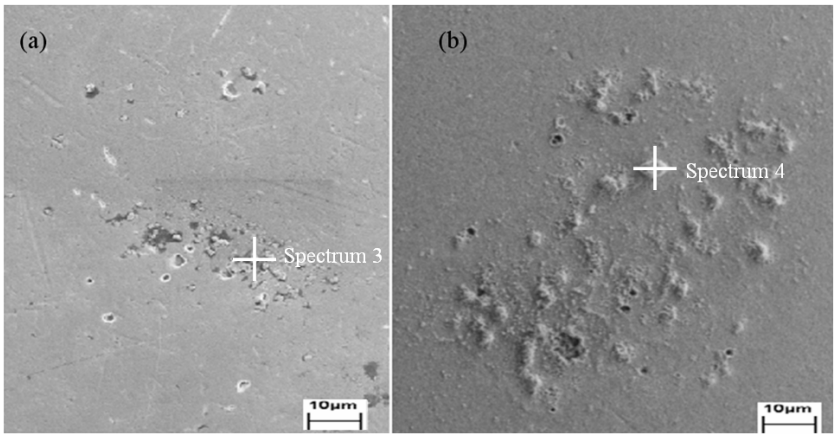

Figure 15: SEM image of (a) Au hemispherical probe for Au-Au/MWCNT contact pair after more than 1 million cycles at current load 1mA, 4V and (b) Au hemispherical probe for Au-Au/MWCNT contact pair at current load 10mA, 4V.

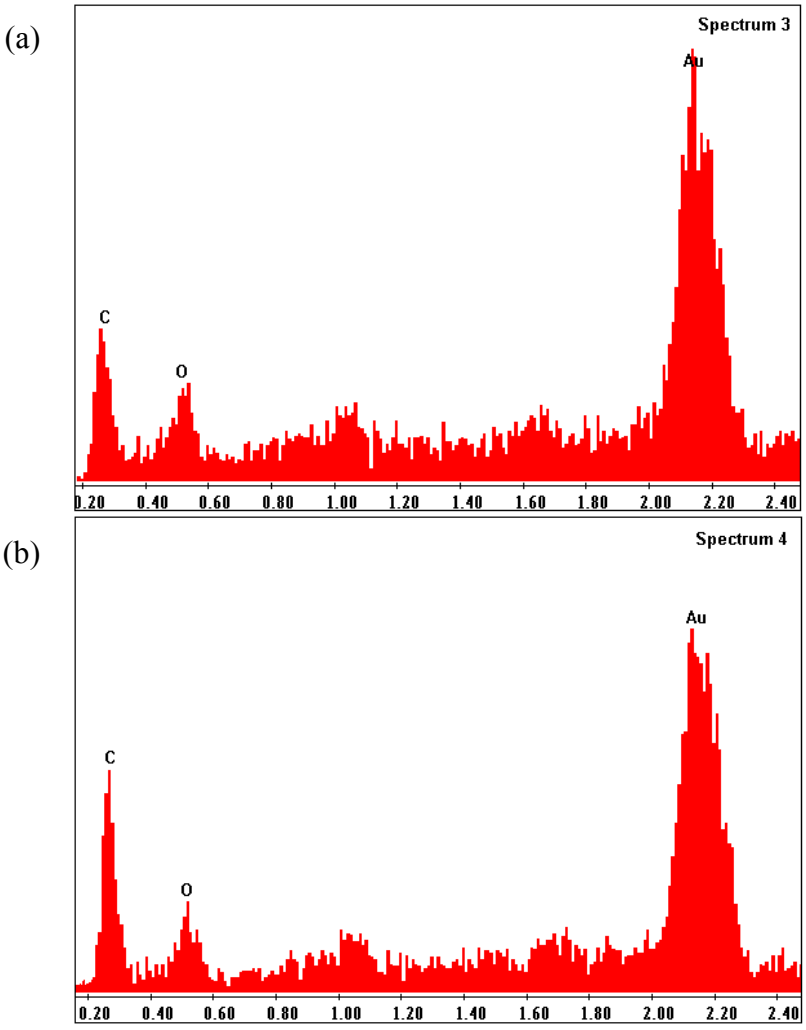

Figure 16: (a) EDX spectrum of Au hemispherical probe surface adhered with Au from the coated Au/MWCNT surfaces (1mA) (b) EDX spectrum of Au hemispherical probe surface adhered with Au from the coated Au/MWCNT surfaces (10mA).

This can be confirmed using X-ray spectroscopy. Fig 15 (a) and (b) shows the points analysed by X-ray spectroscopy on the Au hemispherical probe "Spectrum 3" and "Spectrum 4". Fig 16 (a) and (b) shows an EDX spectrum for the surface. Gold is the

predominantly observed element with carbon and oxygen also observed on both surfaces. This is consistent with the composition of the melted Au and adhered on to the Au hemispherical probe surfaces, with some additional surface contamination and water adsorption. The overall atomic percent of Au is 77.2%, C is 16.78% and O 6.02% for the point "Spectrum 3" and the overall atomic percent of Au is 71.85%, C is 22.78% and O 5.37% for the point "Spectrum 4". Fig 17 also shows an example of a scanned image of the adhered Au on the Au hemispherical probe using TaiCaan (Xyris 4000CL). There are visible protrusion on the surface, these are adhered Au on the Au hemispherical probe surfaces as shown also in Fig 15 and 16, SEM image and chemical compositions respectively.

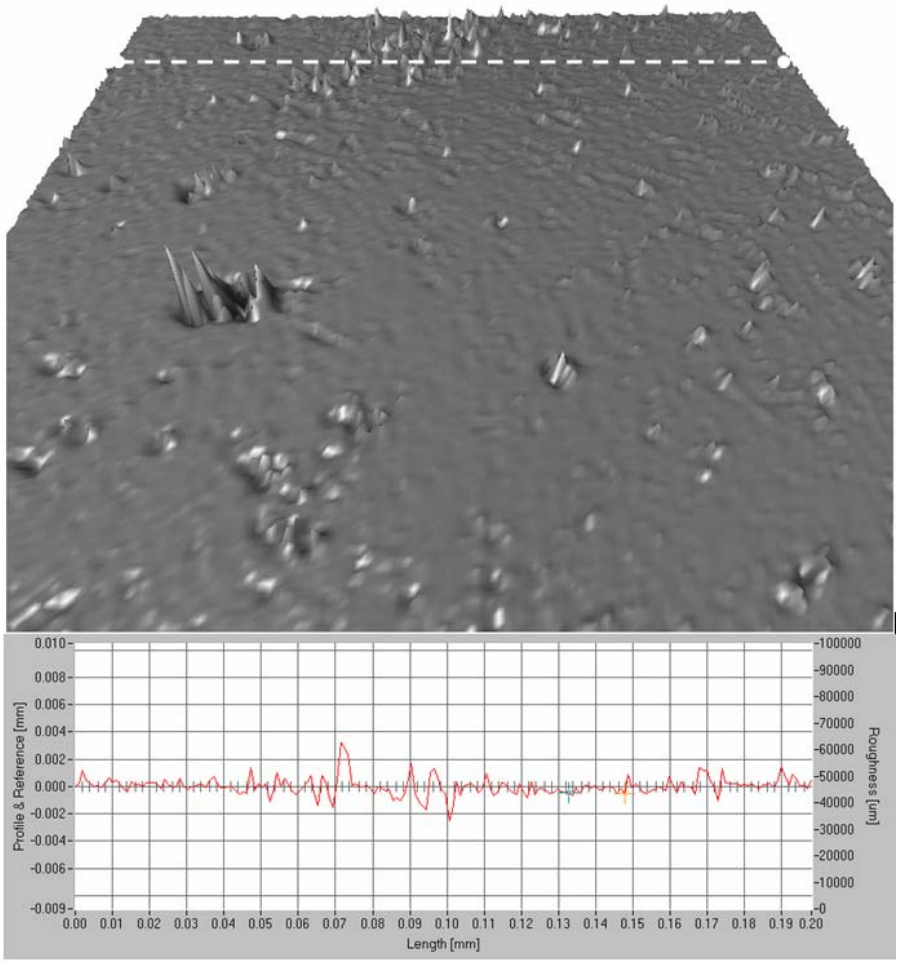

Figure 17: Example of scanned image of adhered Au on the Au hemispherical probe (with sphere removed) from Au/MWCNT surface coating (with current load 10mA) after more than a million cycles, contact pair 201x201 (0.2mmx0.2mm) using TaiCaan (Xyris 4000CL).

No observable damage, deformation or change in chemical composition on Au/MWCNT planar composite surfaces can be detected, further suggesting that the CNT under layer has improved the mechanical integrity of the gold surface. The other probable reason for the stable contact resistance of the Au-Au/MWCNT pair is that the CNT deformation reduces the dynamic forces due to the impact of the Au ball, thus decreasing the tendency of damaging the surfaces. Furthermore, the roughness of Au/MWCNT planar surface could have helped to reduce the tendency of adhesion due

to smoothening of the surfaces, which is one of the major causes of MEMS relay's failure.

5. Conclusion

The applied cyclic load and contact resistance between Au-Au/MWCNT composite contact pairs was investigated using a PZT actuator apparatus at current load of 1mA and 10mA using 4V and R_c measurement methods. This contact pair combination was compared with an Au-Au contact pair. Au-Au contact pair shows degradation over 200 cycles but Au-Au/MWCNT contact pair demonstrated a much more stable contact resistance over 1000 cycle and beyond a million load cycles. This improvement is believed to be due to the elastic deformation of the underlying MWCNTs which reduces the plastic deformation and the roughness of the Au/MWCNT planar surfaces which subsequently reduces the adhesion and damage between the Au contact surfaces.

Acknowledgement

The authors thank Dr. David Smith of the School of Physics and Astronomy, for providing the facilities for developing the MWCNT deposition, and to Mr. Tim Hartley for his dedication in fabricating the test apparatus.

References

[1] Coutu, R. A., Kladitis, P. E., Leedy, K. D. and Crane, R. L., 2004, "*Selecting Metal Alloy Electric Contact Materials for MEMS Switches*," Journal of Micromechanics and Microengineering, (14) pp. 1157-1164.

[2] Lee, H., Coutu, R.A., Mall, S., and Leedy, K.D., 2006, *"Characterization of metal and metal alloy films as contact materials in MEMS switches,"* Journal of Micromechanics and Microengineering, pp.557-563.

[3] Yao, J.J., 2000, *"RF MEMS from a device perspective,"* Journal of Micromechanics and Microengineering, v 10, n 4, pp. R9-38.

[4] Schaffner, J.H., Schmitz, A.E., Tsung-Yuan Hsu, Chang, D.T., Loo, R.Y., and Sievenpiper, D.F., 2003, "Metal *contact RF MEMS switch elements for ultra wideband RF front-end systems,"* IEEE Conference on Ultra Wideband Systems and Technologies, pp. 32-6.

[5] Rebeiz, G.M., 2003, *"RF MEMS Theory, Design, and Technology,"* New Jersey, Wiley.

[6] Varadan, V.K., Vinoy, K.J. and Jose, K.A., 2003, *"RF MEMS and their Applications,"* London, Wiley.

[7] Gao, D., Wijesundara, M. B. J., Carraro, C., Low, C. W., Howe, R. T. and Maboudian, R., 2003, "*High Modulus Polycrystalline 3C-SiC Technology for RF MEMS*," The 2th International Conference on Solid State Sensors, Actuators and Mircosystems, 3D3.4, pp. 1160-1163.

[8] Lian, G. D., Dickey, E. C., Ueno, M. and Sunkara, M. K., 2002, "*Ru-doped Nanostructured Carbon Films*," Diamond and Related Materials, 11, pp. 1890-1896.

[9] Yu, M. F., Lourie, O., Dyer, M. J., Moloni, K., Kelly, T. F. and Ruoff, R.S., 2000, "*Strength and Breaking Mechanism of Multiwalled Carbon Nanotubes Under Tensile Load*," Science, 287(5453), pp. 637 – 640.

[10] Wong EW, Sheehan PE, Lieber CM, 1997 *"Nanobeam Mechanics: Elasticity, Strength, and Toughness of Nanorods and Nanotubes,"* Science, 277, pp. 1971-5.

[11] Qi, H.J., Teo, K.B.K., Lau, K.K.S., Boyce, M.C., Milne, W.I., Robertson, J. and Gleason, K.K., 2003, *"Determination of Mechanical Properties of Carbon Nanotubes and Vertically Aligned Carbon Nanotube forests using Nanoindentation,"* Journal of Mechanics and Physics of Solids, 51, pp. 2213-2237.

[12] Thostenson, E. T., Ren, Z. and Chou, T.W., 2001, "*Advances in the Science and Technology of Carbon Nanotubes and their Composites: A review,*" Composites Science and Technology, 61, pp. 1899-1912.

[13]Hjortstam, O., Isberg, P., Söderholm, S. and Dai, H., 2004, *"Can we achieve ultra-low resistivity in carbon nanotube-based metal composites?"* Journal of Applied Physics A, Materials Science & Processing, 78, pp. 1175-1179.

[14] Tzeng, Y., Chen, Y. and Liu, C., 2003, *"Electrical contacts between carbon-nanotube coated electrodes,"* Diamond and Related Materials, 12, pp. 774-779.
[15] Yaglioglu, O., Hart, A. J., Martens, R. and Slocum, A. H., 2006, *"Method of characterizing electrical contact properties of carbon nanotube coated surfaces,"* Review of Scientific Instruments, 77, pp 095105/1-3.
[16] Yunus, E.M., McBride, J.W., and Spearing, S.M., 2007, *"The Relationship between Contact Resistance and Contact Force on Au coated Carbon Nanotubes surfaces,"* Electrical Contact, Proceedings of The 53rd IEEE Holm Conference on Electrical Contacts, Vol.6.4, pp.167-174.
[17] Yunus, E.M., McBride, J.W., and Spearing, S.M., 2008, Improving the contact resistance at low force using gold coated carbon nanotubes surfaces," Proceedings of the 24th International Conference on Electrical Contacts, Saint-Malo, France, Vol. 13.4, pp. 507-513.
[18] Patton, S.T. and Zabinski, J. S., 2005, *"Fundamental studies of Au contacts in MEMS RF switches,"* Tribology Letters, Vol 18, No.2, pp. 215-230.
[19] Dickrell III, D.J. and Dugger, M. T., 2007, *"Silicone Oil Contamination and Electrical Contact Resistance Degradation of Low-Force Gold Contacts,"* Journal of Microelectromechanical Systems, Vol. 16, No. 1, pp. 24-28.
[20] Gregori, G. and Clarke, D. 2006, "The interrelation between adhesion, contact creep, and roughness on the life of gold contacts in radio-frequency microswitches," Journal of Applied Physics, 100, 094904-1-10.
[21] Slade, P. 1999, "Electrical contacts," New York, Basel, Marcel Dekker, Inc.
[22] Dickrell III, D. J. and Dugger, M. T., 2005, "*The effects of surface contamination on resistance degradation of hot-switched low-force MEMS electrical contacts*," Electrical Contacts 2005 - Proceedings of the Fifty-First IEEE Holm Conference on Electrical Contacts, pp. 255-258.